The relativistic density functional investigations on geometries, electronic and magnetic properties of Ir_n (n=1–13) clusters*

Guo Ping(郭 平)[a)†], Zheng Ji-Ming(郑继明)[b)], Zhao Pei(赵 佩)[a)], Zheng Lin-Lin(郑琳琳)[b)], and Ren Zhao-Yu(任兆玉)[b)‡]

[a)] *Physics Department, Northwest University, Xi'an* 710069, *China*
[b)] *Institute of Photonics & Photon-Technology, Northwest University, Xi'an* 710069, *China*

(Received 27 September 2009; revised manuscript received 30 December 2009)

The Ir_n (n=1–13) clusters are studied using the relativistic density functional method with generalized gradient approximation. A series of low-lying structures with different spin multiplicities have been considered. It is found that all the lowest-energy Ir_n (n=4–13) geometries prefer non-compact structures rather than compact structure growth pattern. And the cube structure is a very stable cell for the lowest-energy Ir_n ($n > 8$) clusters. The second-order difference of energy, the vertical ionization potentials, the electron affinities and the atomic average magnetic moments for the lowest-energy Ir_n geometries all show odd–even alternative behaviours.

Keywords: density functional method, the lowest-energy structures of Ir_n clusters, electronic and magnetic properties

PACC: 3640, 3640B, 3640C

1. Introduction

The free atoms of typical transition metals (TMs) have an incompleted subshell in the low-lying energy states, and the d electrons are responsible for the most interesting properties of these elements as free atoms or in the metallic bulk phase.[1,2] In the past years, many transition metal clusters have been studied both experimentally and theoretically.[3−13] The VIII group TMs, such as iron, cobalt, nickel, ruthenium, rhodium, palladium, osmium, and platinum clusters have been investigated extensively, because of their fundamental importance and potential applications in magnetic materials and chemical catalysis. These studies show that the geometric and electronic structures of TM clusters play important roles in understanding their growth behaviour, associated with catalytic, magnetic, thermal, and optical properties.

Being a central 3rd-row TM, iridium has an electronic structure of $5d^76s^2$ and a face-centred cubic (FCC) crystal structure. Iridium is not easily susceptible to corrosion, which makes it useful for high temperature, high-pressure materials and 'clean' applications.[14,15] The catalytic behaviour of iridium clusters with four and six atoms on solid support was observed.[16−18] In order to understand the catalytic behaviour of iridium clusters, the size-dependent reactivity of the Ir_n clusters with n = 4, 6, 8, and 10 was investigated by Hartree–Fock (HF) methods and effective core potential (ECP) basis sets.[19,20] Iridium clusters have been synthesized by ion exchange with Ir $(NH_3)_5Cl_2{}^+$ cations of NaY zeolite.[21] Moreover, the cluster grows in an ideal process, which is related to geometric structures of different compounds. We can describe the metallic frameworks of iridium complex by arranging them in a sequence of known compounds.[22] R. B. King has proved that some new synthesized iridium carbonyl clusters have fused octahedral and trigonal bipyramid by examining their topologies.[23] So it is very interesting to determine the geometrical and electronic structures of iridium

*Project supported by the National Natural Science Foundation of China for Young Scientists (Grant No. 10904123), the National Natural Science Foundation of China (Grant Nos. 10774118 and 10974152), and the Special Item Foundation of Educational Committee of Shaanxi Province, China (Grant No. 08JK471).
†Corresponding author. E-mail: guoping@nwu.edu.cn
‡E-mail: rzy@nwu.edu.cn
© 2010 Chinese Physical Society and IOP Publishing Ltd

clusters by the first principle method.

Although the geometries of iridium nanoparticles have been investigated recently,[24] their electronic spin states have not been determined yet. Here, we will first give a series of low-lying structures of Ir_n (n=3–13) clusters with different spin multiplicities. On the base of these stable geometries, we discussed the structural growth patterns, relative stabilities, and electronic properties of iridium clusters in detail, including the energy gaps between the highest occupied molecular orbital (HOMO) and the lowest unoccupied molecular orbital (LUMO), vertical ionization potentials (VIPs), vertical electronic affinity (VEAs) and atomic averaged magnetic moments.

2. Computational details

All the calculations are performed by utilizing the local spin density approximation (LSDA)[25] augmented with generalized gradient approximation (GGA) of the exchange functional of Becke[26] and the correlation functional of Perdew[27,28] in the Amsterdam Density Functional (ADF) package.[29] Owing to the importance of the relativistic effect on electronic properties of Ir_n clusters, a combined scalar relativistic (SR) zero order regular approximation (ZORA)[30,31] has been taken into account. Furthermore, the frozen-core triple-zeta basis sets plus polarization functions are employed during our calculations, and the inter-shell orbits of iridium atom are kept frozen up to 4d ($1s^2 2s^2 2p^6 3s^2 3p^6 3d^{10} 4s^2 4p^6 4d^{10}$). In the calculation process, spin-unrestricted calculations are performed until a lowest-energy spin electronic configuration occurs. All the lowest-energy structures of iridium clusters are checked by harmonic vibration frequencies. Additionally, the orbital contributions have been ignored in magnetic moments calculations.

To check the reliability of our method, we have calculated the energies of Ir atom and Ir_2 dimmer. The calculated first ionization potential of Ir atom is 9.43 eV which is comparable to the experimental value of 9.1 eV. The calculated result of Ir_2 shows that Ir–Ir bond length (2.249 Å, 1 Å=0.1 nm) and vibration frequency (280.22 cm^{-1}) of the spin quintet state are very close to the results (from 2.244 Å to 2.287 Å) reported by various computational methods[32−34] as well as the experimental results (2.23 Å, 2.35 Å, 2.25 Å and 280.0 cm^{-1}).[35] In particular, the calculated dissociation energy (2.18 eV/atom) of Ir_2 agrees well with the experimental measurement (2.15 eV/atom).[36]

3. Results and discussions

3.1. Geometries and stabilities

All the calculated low-lying Ir_n (n=4–13) geometries, as well as the corresponding symmetries, magnetic moments are displayed in Fig. 1 and listed in Table 1. According to the total bonding energy from low to high, the low-lying isomers are denoted as na, nb, nc, and so on, where n is the number of Ir atoms.

All possible geometries of Ir_3 cluster have linear and triangle structures. We considered two triangle structures with C_{2v} and D_{3h} symmetries. In Ref. [33], the ground state of Ir_3 is a C_{2v} structure with an apex bond angle of 51.6°, a side length of 2.632 Å, and electronic state $^8A_1$, which is obviously different from D_{3h} one. Here, the optimized C_{2v} geometry (3a) with electronic state $^4B_1$ is very close to the D_{3h} structure (3b), with only an energy deviation of 0.0102 eV. For Ir_4 cluster, compact tetrahedron and open planar square structures are possible isomers. Compared with T_d tetrahedron, its Jahn–Teller distortions, C_{3v} and C_1 tetrahedrons drop very slightly in energy, while a clear energy drop is found in an open planar quadrangle. So the lowest-energy Ir_4 geometry is a square structure (Fig. 1, 4a), which is different from other transition metal clusters.[3,8,13] When Ir_5 clusters are concerned, we selected square pyramid, trigonal bipyramid and trapezoidal planar structures as initial low-lying isomers. As a result, the energy of square pyramid 5a is obviously lower than that of other isomers, which is similar to Rh_5.[11] The planar 5c structure is the least stable structure, so we selected some nonplanar structures as initial low-lying isomers of Ir_6, such as trigonal prism, octahedron, face-capped trigonal bipyramid. Similar to the Rh_6 isomer,[11] the lowest-energy Ir_6 cluster 6a is a well-defined D_{3h} prism structure, and the face-capped trigonal bipyramid 6d is the least stable structure. It suggests that Ir_6 does not favour O_h octahedron as well as compact tetrahedron growth pattern.

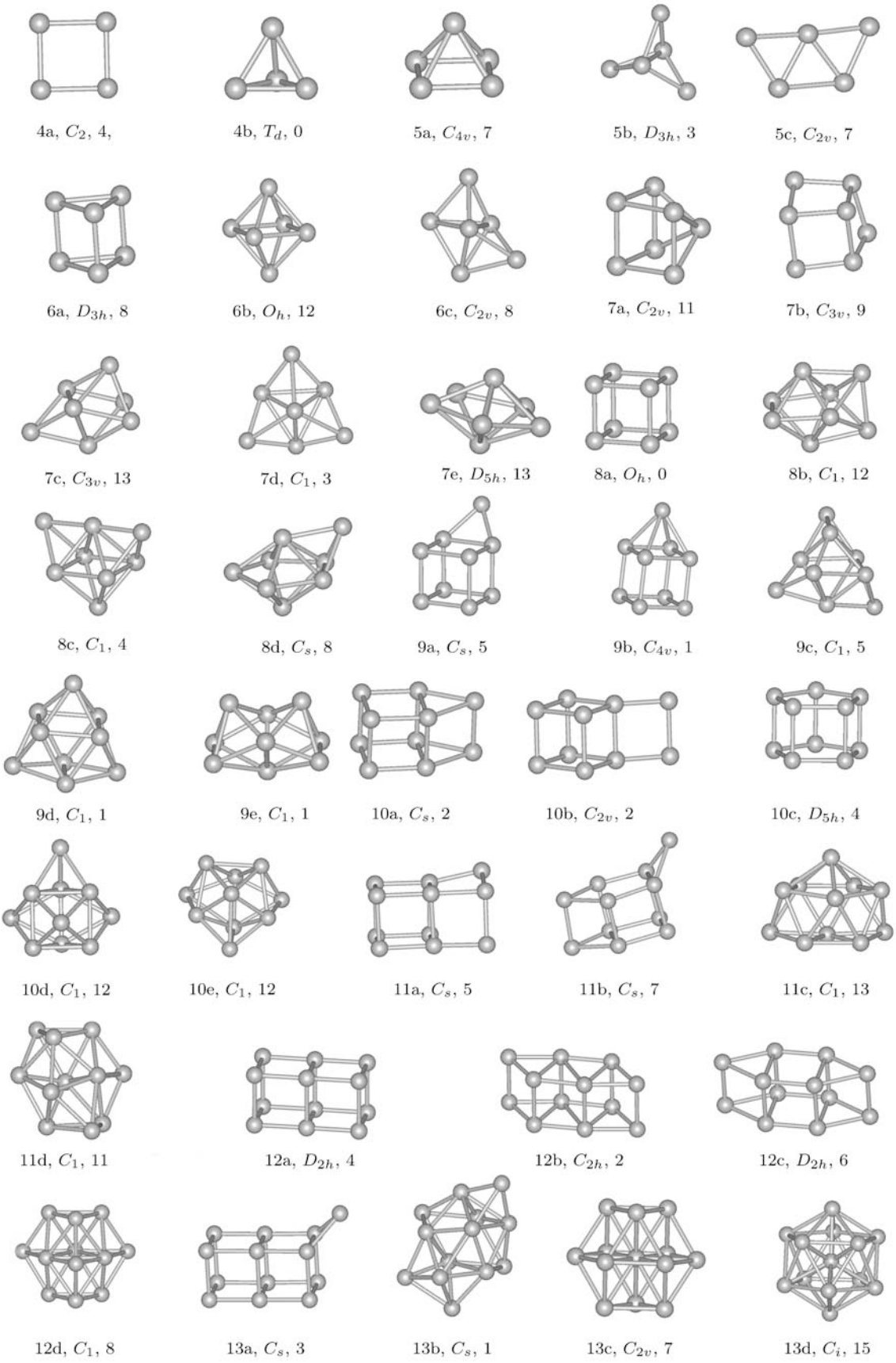


Fig. 1. Low-lying Ir_n geometries (n=4–13), the corresponding point-group symmetries along with the magnetic moments in the unit of μ_B.

Table 1. Isomers, symmetries, magnetic moments (MM), electronic states, total bonding energies (E), the HOMO and LUMO energies and the Ir–Ir bond length range (R) of Ir_n (n=1–13) clusters.

isom	sym	MM/μ_B	E/eV	HOMO/eV	LUMO/eV	R/Å	state
Ir_2							
2a	$D_{\infty h}$	4	–8.2065	–4.4583	–4.2983	2.249	$^5\Delta_g$
Ir_3							
3a	C_{2v}	3	–13.9817	–4.4264	–3.9977	2.399–2.400	$^4B_1$
3b	D_{3h}	3	–13.9715	–4.4264	–4.0053	2.402	$^4E'_1$
Ir_4							
4a	C_2	4	–21.1132	–4.9875	–4.8740	2.540	^5B
4b	T_d	0	–19.8957	–4.0331	–3.5324	2.494	$^1A_1$
Ir_5							
5a	C_{4v}	7	–27.6097	–5.0302	–4.7605	2.431–2.538	$^8A_2$
5b	D_{3h}	3	–26.5868	–4.9478	–4.5476	2.431–2.521	$^4E'$
5c	C_{2v}	7	–26.5438	–4.8475	–4.7309	2.421–2.570	^8B
Ir_6							
6a	D_{3h}	8	–35.2642	–4.9370	–4.6867	2.367–2.491	—
6b	O_h	12	–34.7395	–4.7135	–4.5366	2.563	—
6c	C_{2v}	8	–33.7601	–4.8043	–4.5687	2.520–2.631	$^9A_2$
Ir_7							
7a	C_{2v}	11	–42.0920	–4.7750	–4.6193	2.507–2.569	$^{12}A_2$
7b	C_{3v}	9	–41.8446	–4.9807	–4.7472	2.377–2.436	$^{10}A_1$
7c	C_{3v}	13	–41.1597	–4.9998	–4.7353	2.572–2.599	$^{14}A_1$
7d	C_1	3	–40.8316	–4.7978	–4.6177	2.415–2.877	^4A
7e	D_{5h}	13	–40.5279	–4.6942	–4.4652	2.610–2.693	—
Ir_8							
8a	O_h	0	–51.1507	–5.5206	–5.2418	2.396	$^1A_{1g}$
8b	C_1	12	–48.4466	–4.8029	–4.6042	2.548–2.612	^{13}A
8c	C_1	4	–48.1505	–4.9130	–4.7532	2.465–2.616	^5A
8d	C_1	8	–47.5267	–4.9489	–4.7025	2.470–2.703	^9A
Ir_9							
9a	C_s	5	–57.6001	–4.9535	–4.7604	2.396–2.524	$^6A'_1$
9b	C_{4v}	1	–57.1265	–5.3406	–5.0827	2.405–2.685	$^2A_1$
9c	C_1	5	–55.7813	–4.9410	–4.7690	2.424–2.918	^6A
9d	C_1	2	–55.2341	–4.8522	–4.7456	2.451–2.603	^2A
9e	C_s	1	–54.7435	–4.7987	–4.6941	2.449–2.659	$^2A'$
Ir_{10}							
10a	C_s	2	–65.4217	–5.1680	–4.9722	2.382–2.511	$^3A'$
10b	C_{2v}	2	–65.0832	–5.0240	–4.9101	2.362–2.417	$^3B_2$
10c	D_{5h}	4	–63.8230	–5.1053	–4.9183	2.392–2.415	$^5A'_1$
10d	C_1	12	–62.6789	–4.7558	–4.6892	2.460–2.696	^{13}A
10e	C_1	12	–62.6092	–4.6410	–4.5883	2.495–2.828	^{13}A
Ir_{11}							
11a	C_s	3	–72.2016	–4.9914	–4.7481	2.392–2.438	$^4A''$
11b	C_s	7	–70.9564	–5.1254	–4.8916	2.384–2.755	$^8A'$
11c	C_1	13	–69.5109	–4.7874	–4.6834	2.511–2.730	^{14}A
11d	C_1	11	–69.3808	–4.8621	–4.6958	2.478–2.734	^{12}A
Ir_{12}							
12a	D_{2h}	4	–81.6547	–4.8533	–4.8271	2.427–2.440	^5A_g
12b	C_{2h}	4	–78.6722	–5.1979	–4.9802	2.393–2.916	^5A_g
12c	D_{2h}	6	–78.3156	–5.3142	–5.1814	2.399–2.532	$^7A_{2g}$
12d	C_1	8	–77.4153	–4.8918	–4.7178	2.548–2.890	^9A
Ir_{13}							
13a	C_s	3	–87.7456	–5.0856	–4.8505	2.404–2.515	$^4A'$
13b	C_s	1	–84.6578	–4.9154	–4.7919	2.518–2.817	$^2A'$
13c	C_{2v}	7	–83.1540	–5.2257	–5.1758	2.405–2.552	$^8B_1$
13d	C_i	15	–81.2834	–4.8324	–4.7044	2.567–2.769	^{16}A

As the cluster size rises, the isomer number increases rapidly. Guide by some above and previous theoretical or experimental results,[11,12] we considered some typical low-lying structures for Ir_7 and Ir_8 clusters. These low-lying Ir_7 isomers are ordered by the energy from low to high as follows: the face-capped prism 7a, the edge-capped prism 7b, the capped octahedron 7c, the tri-capped tetrahedron 7d, and the pentagonal bipyramid 7e. The stability orders of Ir_8 isomers are the cube 8a, the Ir_2 dimer capped octahedron 8b, the two separated Ir atoms capped octahedron 8c, and the capped pentagonal bipyramid 8d in turn. Analogous to Rh_8^{11} and Ni_8^{12} clusters,[11,12] the lowest-energy 8a isomer is a non-compact O_h symmetry cubic structure, but it is nonmagnetic, which is different from Ni_8 and Rh_8, with 4 μ_B and 12 μ_B magnetic moments respectively. The 8a is much lower than other isomers in energy, ascribed to not only its close-shell electronic configuration, but also its electrons occupying the lower-energy molecular orbitals. Its HOMO energy (−5.521 eV in Table 1), for instance, is obviously lower than that of the other most stable Ir_n clusters. Here, the high symmetrical D_{5h} pentagonal bipyramid is the least stable structure in Ir_7 isomers.

Based on the above discussions, we mainly considered some low-lying combinations of small clusters from Ir_9 to Ir_{13}. All considered Ir_9 isomers are as follows: the edge-capped cube 9a, the face-capped cube 9b, the tricapped octahedron 9c, the tricapped trigonal prism 9d, and the fused octahedron 9e. Surprisingly, it was found that the edge-capped cube C_s (9a) is lower than the face-capped cube C_{4v} (9b) isomer in energy, which possibly attributes to the orientation of the d-bands for the most part.[12] For Ir_{10} clusters, we considered the fusion structure of cube and trigonal prism 10a, the edge-bicapped cube 10b, the regular pentagon prism 10c, the tetracapped trigonal prism 10d, and the fused octahedron 10e. The 10a with C_s symmetry can be viewed as a fusion of the lowest-energy Ir_6 and Ir_8. The lowest-energy Ir_{11} isomer (11a) was obtained by removing an atom from 12a structure. As for Ir_{12} clusters, the low-lying isomers are ordered according to the energy in this sequence: the fused cube 12a, the fused trigonal prism 12b, the prolate prism 12c (which can be viewed as a combination of one cube and two triagonal prisms) and the layer-like 12d. Ir_{13} has a special atom number, and its typical isomers are generally icosahedrons and cuboctahedrons, and so on. However, when several possible low-lying Ir_{13} isomers are optimized, the results show that 13a still keeps a hollow structure and a cube-cell pattern.

3.2. Structural growth pattern and relative stabilities

Based on the available low-lying Ir_n structures presented above, we find that all the lowest-energy Ir_n (n=4–13) geometries are in favour of noncompact hollow structures, instead of compact tetrahedrons, octahedrons or icosahedrons growth patterns. The cube structure is a very stable cell to build larger Ir_n clusters ($n > 8$). For example, 9a is an edge-capped cube, 10a is a bicapped cube, and 12a is a fusion of two cubes, while 11a and 13a can be obtained from 12a structure. In addition, there are other growth patterns in low-lying Ir_n structures, 9d and 10d are typical trigonal prism pattern, and the layer-like 11d, 12d and 13c structures are considered as FCC fragments. Alternatively, 7c, 8b, 9e and 10e isomers show an octahedron growth, but they are not the most stable isomers, which imply a quantum size effect to be taken into account.

In order to compare relative stabilities of the most stable Ir_n (n=2–13) clusters, the averaged binding energy ($E_b(n)$) and second-order difference of energies $\Delta_2 E(n)$ are calculated as follows:

$$E_b(n) = (nE_{atom} - E(n))/n,$$
$$\Delta_2 E(n) = E(n+1) + E(n-1) - 2E(n),$$

where $E(n)$ and E_{atom} represent the total bonding energy of Ir_n cluster and the atomic energy of Ir atom respectively. E_{atom} is calculated for −1.92 eV. The calculated results of averaged binding energy ($E_b(n)$) (Table 2) and second-order difference of energies $\Delta_2 E(n)$ of the lowest-energy Ir_n clusters are shown in Figs. 2 and 3 and listed in Table 2. As indicated in Fig. 2, the averaged BE climbs with the cluster size and some small fluctuated peaks could be found for the even number of n. The dramatic odd–even alternative behaviour is shown in the curve of $\Delta_2 E(n)$ versus the cluster size (Fig. 3), indicating that the even-sized Ir_n clusters are relatively more stabler than the neighbouring odd-sized ones. Especially, both Ir_8 and Ir_{12} clusters are remarkably stable than their neighbour clusters.

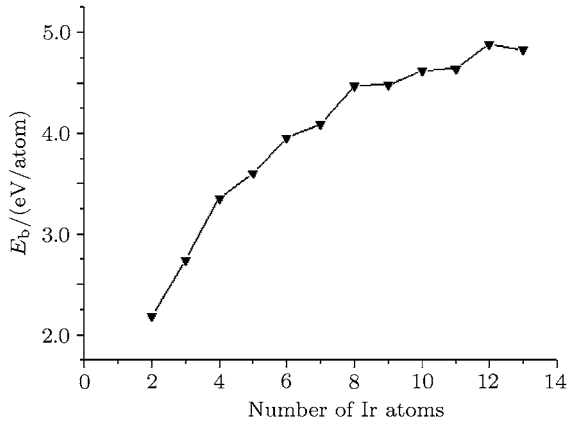


Fig. 2. Size dependence of average binding energies ($E_b(n)$) on the lowest-energy Ir_n clusters.

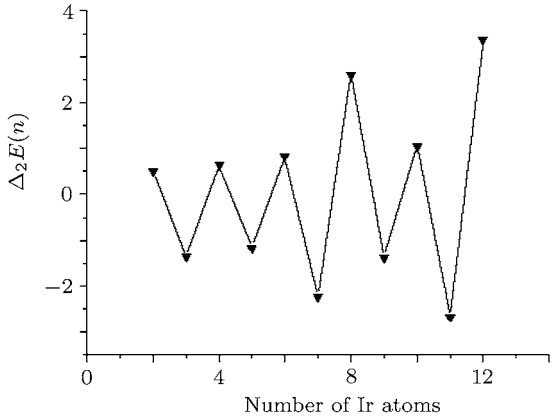


Fig. 3. Size dependence of the second-order differences $\Delta_2E(n)$ on total bonding energy of the lowest-energy Ir_n clusters.

Table 2. Atomic averaged binding energies (BE), HOMO–LUMO gaps (L–H gap), averaged atomic magnetic moments (MM), vertical ionization potentials (VIP), and vertical electronic affinities (VEA) of the most stable Ir_n clusters.

cluster	isomer	state	BE/(eV/atom)	L–H gap/eV	MM/(μ_B/atom)	VIP/eV	VEA/eV
Ir_2	2a	$^5\Delta_g$	2.183	0.1600	2.0	8.593	1.728
Ir_3	3a	$^4B_1$	2.741	0.4287	1.0	7.589	1.864
Ir_4	4a	^5B	3.358	0.1135	1.0	7.242	2.706
Ir_5	5a	$^8A_2$	3.601	0.2597	1.4	7.150	2.462
Ir_6	6a	$^9E_1''$	3.957	0.2667	1.33	7.269	2.433
Ir_7	7a	$^{12}A_2$	4.093	0.1557	1.57	6.905	2.348
Ir_8	8a	$^1A_{1g}$	4.473	0.2788	0.0	7.406	3.179
Ir_9	9a	$^6A_1$	4.480	0.1931	0.56	6.897	2.838
Ir_{10}	10a	$^3A'$	4.622	0.1958	0.2	6.975	3.120
Ir_{11}	11a	$^4A''$	4.643	0.2433	0.27	6.801	2.978
Ir_{12}	12a	^5A_g	4.884	0.0262	0.17	6.782	2.982
Ir_{13}	13a	$^4A'$	4.829	0.2351	0.23	6.721	3.047

3.3. Electronic structures

The energy gap between HOMO and LUMO is an interesting parameter of the electronic structure. A large HOMO–LUMO gap indicates that the cluster is chemically stable, whereas a small gap shows that the cluster is chemically active**.** As seen from Table 2, the HOMO–LUMO gaps of most Ir_n clusters are small and below 0.3 eV, and Ir_3 has the largest HOMO–LUMO gap of 0.43 eV, which indicates Ir_3 is chemically stable. Figure 4 shows size dependence of the HOMO–LUMO gaps of the lowest-energy Ir_n clusters, where a slight oscillation phenomenon with cluster size occurs. Interestingly, Ir_8 has the largest HOMO–LUMO gap among Ir_n ($n > 6$) clusters, which further suggests that it is chemically stable cell to build larger clusters.

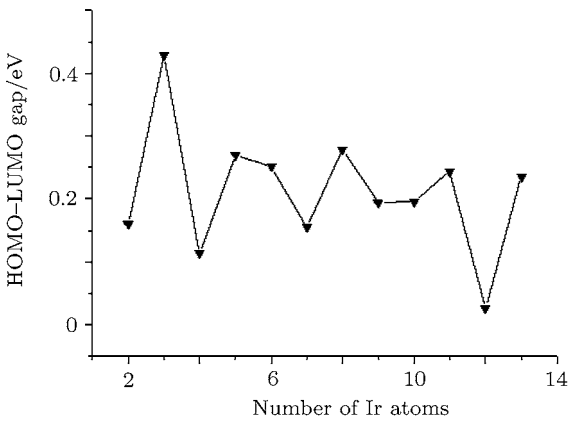


Fig. 4. Size dependence of the HOMO–LUMO gaps on the lowest-energy Ir_n clusters.

On the other hand, vertical electronic affinities ionization potentials (VIP) and vertical ionization potentials (VEA) of the cluster reflects the abilities to lose and obtain an electron respectively. The calculated VIPs (Fig. 5) for the lowest-energy Ir_n clusters have shown odd–even oscillation features between $n = 4$ and $n = 13$, and the even-sized clusters have higher VIPs than their neighbours, indicating that the even-sized Ir_n clusters are relatively more stable than the neighbouring odd-sized ones. The similar result can be concluded from VEAs (Fig. 6). Especially, the VIP of Ir_8 behaves just the same way as that the VEA does, namely, they have obviously higher value at a very close atom number.

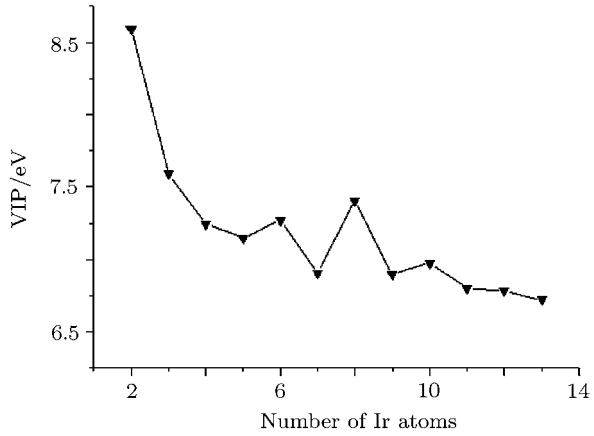


Fig. 5. Size dependence of the vertical ionization potentials (VIPs) on the lowest-energy Ir_n clusters.

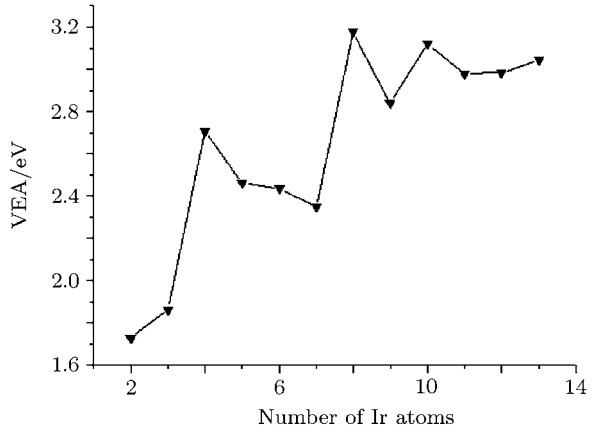


Fig. 6. Size dependence of the vertical electronic affinities (VEAs) on the lowest-energy Ir_n clusters.

3.4. Magnetic properties

The magnetic moments of Ir_n clusters depend on their geometries and spins. The tetrahedron (4b) and cubic 8a structures are nonmagnetic, while the planar square (4a) and the dimer capped octahedron isomers (8b) have a magnetic moment of 4 μ_B and 12 μ_B respectively. The icosahedron 13e is unfavourable in energy, but it has a high magnetic moment 15 μ_B. Figure 7 shows the size dependence of the atomic average magnetic moments on the lowest-energy Ir_n clusters. The magnetic moment per atom decreases with the cluster size increasing, and the small-sized Ir_n ($n < 8$) clusters have large average magnetic moments of $\bar{\mu} \geq 1.0$ μ_B/atom. The odd–even oscillation occurs between $n = 4$ and $n = 13$, which matches the stability characteristics of Ir_n (n=4–13) clusters. It is implied that an antiferromagnetic electron order exists in these non-compact lowest-energy iridium clusters.

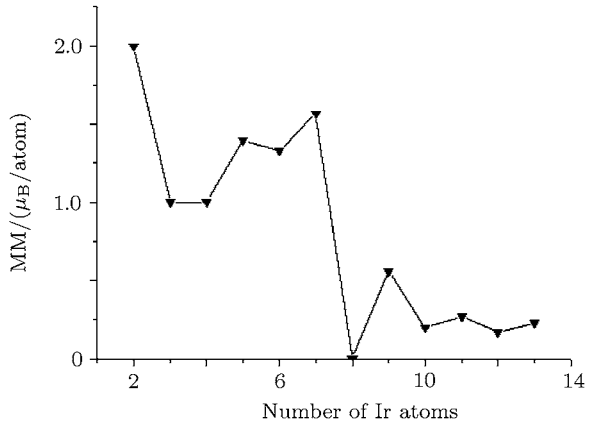


Fig. 7. Size dependence of the average atomic magnetic moments on the lowest-energy Ir_n clusters.

4. Conclusions

The electronic structures of the small-sized Ir_n (n=1–13) clusters are investigated by relativistic density functional theory (RDFT) with the generalized gradient approximation (GGA) by considering the exchange–correlation energy available in ADF. All the lowest-energy Ir_n (n=4–13) geometries do not support compact structure growth pattern, but favour open structures. The cube cell is a part of larger clusters ($n > 8$). Also, trigonal prism, FCC fragment and octahedron growth patterns are found in low-lying Ir_n clusters. The odd–even oscillation features of the lowest-energy structures are shown in the second-order energy differences, the VIPs, the VEAs, which indicate that the even iridium clusters are more stable than the neighbouring odd ones. The LUMO–HOMO gaps of these iridium clusters are universally small. In addition, the atomic average magnetic moment decreases with the cluster size increasing, and the small-sized Ir_n clusters ($n < 8$) have larger magnetic moments of $\bar{\mu} \geq 1.0$ μ_B/atom. The magnetic mechanism of iridium clusters is expected to be further study.

References

[1] Alonso J A 2000 *Chem. Rev.* **100** 637
[2] Baletto F and Ferrando R 2005 *Rev. Mod. Phys.* **77** 371
[3] Luo Y H, Ren F Z, Wang Y X, Wei S K and Zhang G B 2009 *Chin. Phys.* B **18** 1491
[4] Lei X L, Luo Y H, Wang X M and Zhu H J 2009 *Chin. Phys.* B **18** 2264
[5] Feng C J, Xue Y H, Zhang X C and Zhang X Y 2009 *Chin. Phys.* B **18** 1436
[6] Bobadova-Parvanova P, Jackson K A, Srinivas S and Horoi M 2005 *J. Chem. Phys.* **122** 014310
[7] Wang J L, Wang G H and Zhao J J 2002 *Phys. Rev.* B **66** 035418
[8] Kumar V and Kawazoe Y 2002 *Phys. Rev.* B **65** 125403
[9] Bucher J P, Doaglass D C and Bloomfield L A 1991 *Phys. Rev. Lett.* **66** 3052
[10] Deng K M, Yang J L, Xiao C Y and Wang K L 1996 *Phys. Rev.* B **54** 2191
[11] Bae Y C, Osanai H, Kumar V and Kawazoe Y 2004 *Phys. Rev.* B **70** 195413
[12] Reuse F A, Khanna S N and Bernel S 1995 *Phys. Rev.* B **52** R11650
[13] Zhao W J, Lei X L, Yan Y L,Yang Z and Luo Y H 2007 *Acta Phys. Sin.* **56** 5209 (in Chinese)
[14] Baldo M A, Thompson M B and Forrest S R 2000 *Nature* (London) **403** 750
[15] Habar, Ouannasser S, Stauffer L, Dreyssé H and Wille L T 1996 *Surf. Sci.* **5** 352
[16] Xu Z, Xiao F S, Purnell S K, Alexeev O, Kawi S, Deutsch S E and Gates B C 1994 *Nature* **372** 346
[17] Maloncy S D, van Zon F B M, Kelley M J, Koningsbegger D C and Gates B C 1990 *Caral. Lett.* **5** 161
[18] Xiao F S, Xu Z, Alexeev O and Gates B C 1995 *J. Phys. Chem.* **99** 1548
[19] Hay P J and Wadt W R 1985 *J. Chem. Phys.* **82** 299
[20] Feng J N, Huang X R and Li Z X 1997 *Chem. Phys. Lett.* **276** 334
[21] Zhao A, Jensoft R E and Gates B C 1997 *J. Cata.* **169** 263
[22] Pergola R D, Garlaschelli L, Manassero M and Sansoni M 1999 *J. Clust. Sci.* **10** 109
[23] King R B 2002 *Inorganica Chimica Acta* **334** 34
[24] Pawluk T, Hirata Y and Wang L C 2005 *J. Phys. Chem.* B **109** 20817
[25] Vosko S H, Wilk L and Nusair M 1980 *Can. J. Phys.* **58** 1200
[26] Becke A D 1988 *Phys. Rev.* A **38** 3098
[27] Perdew J P 1986 *Phys. Rev.* B **33** 8822
[28] Perdew J P 1986 *Phys. Rev.* B **34** 7406
[29] Velde G Te and Baerends E J 1992 *J. Comput. Phys.* **99** 84
[30] Lenthee E van, Bearends E J and Snijders J G 1994 *J. Chem. Phys.* **101** 9783
[31] Lenthee E van, Snijders J G and Bearends E J 1996 *J. Chem. Phys.* **105** 6505
[32] Wu Z J, Han B, Dai Z W and Jin P C 2005 *Chem. Phys. Lett.* **403** 367
[33] Dai D G, Liao M Z and Balasubramanian K 1996 *Chem. Phys. Lett.* **249** 141
[34] Venturelli A and Rauchfuss T B 1994 *J. Am. Chem. Soc.* **116** 4824
[35] Jules J L and Lombardi J R 2003 *J. Phys. Chem.* A **107** 1268
[36] Miedema A R and Gingerich K A 1979 *J. Phys.* B: *At. Mol. Phys.* **12** 2081